Remote Sensing of Environment xxx (2016) xxx–xxx

Contents lists available at ScienceDirect

Remote Sensing of Environment

journal homepage: www.elsevier.com/locate/rse

SMOS optical thickness changes in response to the growth and development of crops, crop management, and weather

Brian K. Hornbuckle [a,*], Jason C. Patton [a,1], Andy VanLoocke [a], Andrew E. Suyker [b], Matthew C. Roby [a], Victoria A. Walker [a], Eswar R. Iyer [a,2], Daryl E. Herzmann [a], Erik A. Endacott [a]

[a] Iowa State University of Science and Technology, Ames, IA, USA
[b] University of Nebraska, Lincoln, NE, USA

ARTICLE INFO

Article history:
Received 4 August 2015
Received in revised form 15 February 2016
Accepted 18 February 2016
Available online xxxx

Keywords:
Passive microwave remote sensing (microwave radiometry)
Soil Moisture and Ocean Salinity (SMOS)
L-band
Optical thickness
Vegetation
Agriculture
Annual crops
Corn (maize)
Soybean

ABSTRACT

The Soil Moisture and Ocean Salinity (SMOS) remote sensing satellite was launched by the European Space Agency in 2009. The L-band brightness temperature observed by SMOS has been used to produce estimates of both soil moisture and τ, the optical thickness of the land surface. Although τ should theoretically be proportional to the amount of vegetation present within a SMOS pixel, several initial investigations have not been able to confirm this expected behavior. However, when the noise in the SMOS τ product is removed, τ in the U.S. Corn Belt, a region of extensive row-crop agriculture, has a distinct shape that mirrors the growth and development of crops. We find that the peak value of SMOS τ occurs at approximately 1000 °C day (base 10 °C) growing degree days after the mean planting date of maize (corn). We can explain this finding in the following way: τ is directly proportional to the water column density of vegetation; maize contributes the most to growing season changes in τ in the Corn Belt; and maize reaches its maximum water column density at its third reproductive stage of development, at about 1000 °C day growing degree days. Consequently, SMOS τ could be used to monitor the phenology of crops in the Corn Belt at a spatial resolution similar to a U.S. county and a temporal frequency on the order of days. We also examined the magnitude of the change in SMOS τ over the growing season and hypothesized it would be related to the amount of accumulated solar radiation, but found this not to be the case. On the other hand, the change in magnitude was smallest for the year in which the most precipitation fell. These findings are rational since SMOS τ at the satellite scale is in fact a function of both vegetation and soil surface roughness, and soil surface roughness is reduced by precipitation. To fully explain changes in SMOS τ in the Corn Belt it appears that it will be necessary to use in situ and remotely-sensed observations along with agro-ecosystem models to account for land management decisions made by farmers that affect changes in soil surface roughness and all of the relevant biophysical processes that affect the growth and development of crops.

© 2016 Elsevier Inc. All rights reserved.

1. Introduction

The European Space Agency's Soil Moisture and Ocean Salinity (SMOS) satellite remote sensing mission employs passive microwave remote sensing to monitor Earth through the use of an L-band (f = 1.4 GHz, λ = 21 cm) radiometer (Kerr et al., 2010). At microwave frequencies liquid water has a high dielectric constant (Grant, Buchanan, & Cook, 1957) making it distinct from most other natural materials. At L-band vegetation is semi-transparent and consequently Earth's terrestrial brightness temperature is sensitive to the water content of the first few cm of the soil surface (e.g., Escorihuela, Chanzy, Wigneron, & Kerr, 2010). In view of other microwave sensors currently in orbit, L-band is considered to be the optimum frequency for soil moisture remote sensing because of its long wavelength.

While semi-transparent, the influence of vegetation on measured brightness temperature is the single most important factor that affects the retrieval of soil moisture (e.g., Holmes, Drusch, Wigneron, & de Jeu, 2008). It is interesting to note that the sensitivity of L-band brightness temperature, T_B, to weakly-scattering vegetation is nearly the same as the sensitivity to soil moisture, θ_v. Using the model that forms the basis for the SMOS retrieval algorithm (Wigneron et al., 2007), it can be shown that $\partial T_B/\partial\theta_v \approx -2.5$ K per 0.010 m^3 m^{-3} when τ, the optical thickness of a vegetation canopy, which quantifies the degree to which vegetation attenuates propagating radiation, is 0.10 Np or equivalent to a knee-high maize (corn) canopy (Hornbuckle, England, De Roo, Fischman, & Boprie, 2003). When τ increases to 0.40 Np (a chest-high maize canopy), $\partial T_B/\partial\theta_v \approx -1.1$ K per 0.010 m^3 m^{-3}. On the other hand, when θ_v = 0.40 m^3 m^{-3} (a wet soil), $\partial T_B/\partial\tau \approx 2.2$ K per 0.010 Np, and when θ_v = 0.10 m^3 m^{-3} (a dry soil), $\partial T_B/\partial\tau \approx 1.0$ K per 0.010 Np.

* Corresponding author.
E-mail address: bkh@iastate.edu (B.K. Hornbuckle).
[1] Now at Oklahoma State University, Stillwater, OK, USA.
[2] Now at the University of Oklahoma, Norman, OK, USA.

http://dx.doi.org/10.1016/j.rse.2016.02.043
0034-4257/© 2016 Elsevier Inc. All rights reserved.

Please cite this article as: Hornbuckle, B.K., et al., SMOS optical thickness changes in response to the growth and development of crops, crop management, and weather, *Remote Sensing of Environment* (2016), http://dx.doi.org/10.1016/j.rse.2016.02.043

Fortunately soil moisture and vegetation generally have opposite effects (as shown above), especially in the case of weakly-scattering vegetation (which is what is assumed by the SMOS retrieval algorithm): an increase in θ_v (with no change in other variables) decreases T_B; while an increase in τ (again with no change in other variables) *increases* T_B. The SMOS team developed a solution to this problem of competing influences by designing an instrument that could retrieve both variables, θ_v and τ, simultaneously. This is accomplished through the use of multiple measurements of T_B at a variety of incidence angles θ to quantify the effect of vegetation on propagating radiation as the observed path length through the canopy changes with θ.

While the vast majority of the focus of the SMOS mission during its first half-decade of operation has been on soil moisture, the SMOS Level 2 τ product may also prove to be useful and perhaps more attention should be paid to this vegetation data product. Some work relating τ to large-scale changes in vegetation has been done at higher microwave frequencies. Jones, Jones, Kimball, and McDonald (2011) retrieved τ (which they call the vegetation optical depth, or VOD) from T_B at 18.7 GHz observed by AMSR-E to examine global phenology. They found that τ compared well with leaf area index (LAI) and visible and near-infrared vegetation indices from MODIS for 82% of Earth's surface. The highest correlations were found for lower amounts of vegetation (e.g., savannas). Recently Liu et al. (2015) used τ (VOD) from SSM/I, AMSR-E, MWRI, and Windsat to estimate changes in aboveground biomass carbon (ABC) in both forests and other ecosystems. Their observations indicated that ABC decreased from 1993 to 2003, but there has been an overall gain in ABC over the last two decades.

It has been shown empirically that τ is directly proportional to the mass of water contained within vegetation tissue per ground area, also called the water column density of vegetation (Jackson & Schmugge, 1991). Therefore τ should be a measure of the amount of growing vegetation within a satellite pixel. While some work has been done with L-band τ from SMOS, these initial investigations have not been able to confirm this expected behavior. For example, Jackson et al. (2012) examined τ in the Little Washita watershed, an area of mainly rangeland in the state of Oklahoma, and found no seasonal pattern. SMOS τ is expected to mirror the growth and senescence of vegetation, especially in agricultural regions. Wigneron et al. (2012) investigated SMOS τ in Spain at the Valencia Anchor Station, a site consisting of mostly vineyards, orchards, shrubs, and scattered pine trees, and found higher values in the winter than in the summer. Schlenz, dall'Amico, Mauser, and Loew (2012) evaluated SMOS τ in an agricultural area in southern Germany. They found τ to be highly variable and to not exhibit a clear seasonal pattern. The average value of τ was higher than expected and positively correlated with SMOS retrieved soil moisture. Bircher, Skou, and Kerr (2013) examined SMOS τ in an agricultural watershed in western Denmark and found it to be noisy and too high on average. The expected seasonal trend of increasing τ during the summer season was faint.

Two investigations of the use of SMOS τ to characterize forested areas achieved some positive results. Rahmoune, Ferrazzoli, Kerr, and Richaume (2013) developed a new version of the SMOS retrieval algorithm customized for forests. They generated two global maps of τ using data from the beginning of July and November, 2011, and found that forested areas had larger τ values than non-forested areas. They also found, as expected, that there was little seasonal change in τ for forests. This work was continued by Rahmoune et al. (2014) who compared SMOS forest τ with LIDAR-estimated forest height from the ICEsat satellite. They added two more time intervals in 2011 (February and May) and found that τ increased as mean forest height increased in each time interval. There was little difference in τ among the four time intervals. One caveat to this work is that there was a six-year time difference between the SMOS and LIDAR data.

Lawrence et al. (2014) revisited the behavior of SMOS τ in agricultural regions. They compared τ with MODIS vegetation indices for approximately 500 SMOS pixels in the U.S. Midwest for which crops were the dominant landcover type, over a two-year period, from 2010 to 2011. The indices investigated were the MODIS Normalized Difference Vegetation Index (NDVI), the MODIS Enhanced Vegetation Index (EVI), MODIS LAI, and a custom normalized difference water index (NDWI) generated from other MODIS observation bands. They also found SMOS τ to be noisy, with variations between 0.2 and 0.5 Np in August for pixels with greater than 0.9 crop fraction. Coefficient of determination (R^2) values of only 0.32 to 0.35 were found for all comparisons of τ with each vegetation index. Higher R^2 values were found for pixels which had more maize and soybean and lower values for pixels with wheat and hay. On the other hand, τ and LAI values started to increase at the same point in the growing season. The peak value of τ occurred about 19 days later than the peak of LAI, consistent with the fact that τ is sensitive to all canopy components and not just leaves. NDVI, EVI, and NDWI reached saturation points during the growing season (values plateaued and did not increase further) but τ and LAI did not.

It is certainly true that SMOS Level 2 τ data currently available from the European Space Agency is quite noisy: large swings from relatively small to large values occur over short periods of time, sometimes on consecutive days. It is not known at present what causes this noise. Another complicating factor is that τ retrieved from satellite observations actually depends on both the amount of vegetation and the roughness of the soil surface (Njoku & Chan, 2006; Patton & Hornbuckle, 2013). The SMOS retrieval algorithm currently assumes a static soil surface roughness but in reality it changes over time, especially in agricultural areas. Management such as tillage increases soil surface roughness, while subsequent rainfall erodes and decreases it. Because of the noisiness of τ data, the geographic locations in which it has been investigated, and potentially significant time-varying signals of soil surface roughness, it is perhaps not so surprising that SMOS τ has not met expectations, especially since the SMOS mission has to date focused on soil moisture retrieval and validation, and not on the retrieval and validation of optical thickness.

In the U.S. Corn Belt, however, the seasonal variation of vegetation is large and a pattern does emerge from the noise. The majority of land area in the Corn Belt is devoted to annual crops, primarily maize (corn) and soybean. Patton and Hornbuckle (2013) found that a running average of SMOS λ increased in the late spring and early summer as crops grew, and decreased in the fall as crops senesced (slowly dried out and died) and were harvested. Besides sizable changes in the amount of vegetation within an individual growing season, there should also be significant changes in the year-to-year timing of the growth and development of vegetation in the Corn Belt due to variability in when various crop management practices, such as spring tillage and the planting of crops, occur. This is illustrated by Fig. 1 which shows the percentage of the total acres of maize planted in the Corn Belt state of Iowa during each week of the spring for the past 37 years. Tillage often precedes planting, and both tillage and planting cannot be performed when the soil is too wet. Wet springs can significantly delay crop management, sometimes until farmers are forced to plant different types of crops that can mature in less time. Weather variability over only the past six years has caused the date on which the majority of maize was planted to vary by up to a month. This variability should be evident in SMOS τ data.

Here we investigate how SMOS τ changes from year-to-year in the Corn Belt. Our over-arching hypothesis is that we can both qualitatively and quantitatively explain its year-to-year variability. We test two specific hypotheses in this investigation. First, since τ is most sensitive to the water contained within vegetation tissue (Ulaby & El-Rayes, 1987; Ulaby & Jedlicka, 1984), we hypothesize that the time at which SMOS τ reaches a maximum value during the growing season corresponds to the time that crops reach the developmental stage at which the maximum amount of water per unit ground area is contained within the vegetation. Or in other words, we believe that we can explain the timing of the maximum value of τ over the growing season. And second, we

Please cite this article as: Hornbuckle, B.K., et al., SMOS optical thickness changes in response to the growth and development of crops, crop management, and weather, *Remote Sensing of Environment* (2016), http://dx.doi.org/10.1016/j.rse.2016.02.043

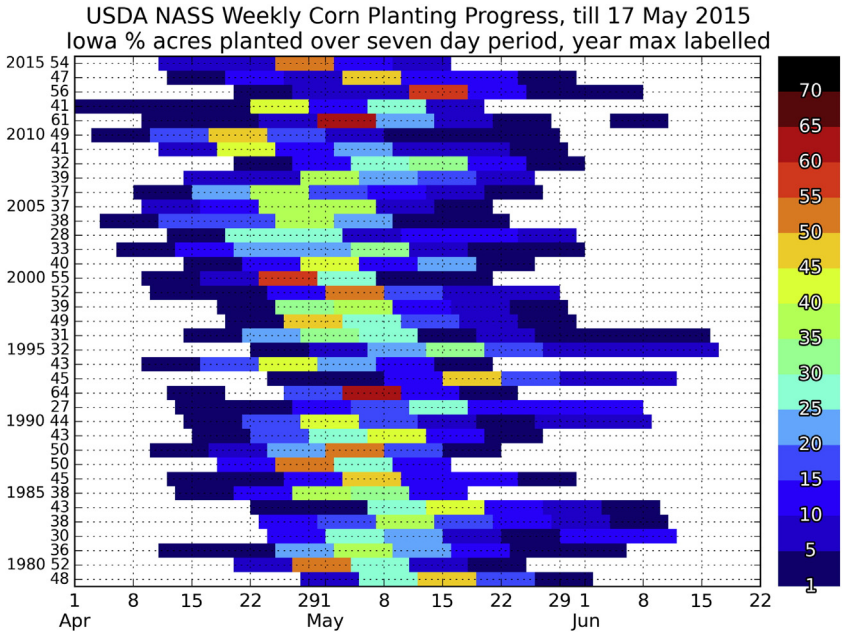

Fig. 1. Variation in date of planting of maize in terms of percentage of total acres planted in each week of spring over the past 37 years in Iowa according to USDA NASS Crop Progress and Condition Reports.

hypothesize that the increase in τ over the growing season (defined as the difference between the maximum τ observed and the value of τ at the beginning of the growing season) is directly related to the growth of crops which is in turn related to the amount of solar radiation accumulated from when crops emerge from the soil to the time of the maximum value of τ. Or in other words, we believe that we can explain the magnitude of the maximum value of τ over the growing season.

2. Materials and methods

2.1. SMOS optical thickness

In order to minimize the influence of vegetation other than crops on τ we only considered SMOS footprints in Iowa, a state in the Corn Belt, that had the highest percentages of land area devoted to annual crops. We used data from the United States Department of Agriculture (USDA) National Agricultural Statistics Service (NASS) Cropland Data Layer (Boryan, Yang, Mueller, & Craig, 2011) and the SMOS Level 2 soil moisture product version 5.5.1. We did not attempt to account for the effect of small lakes (which may alter the magnitude of τ but not the change in τ from year-to-year), and we did not use flags to filter the data, but we did not use τ retrievals when there was no corresponding soil moisture retrieval or when there was no estimate of τ data quality. Since SMOS observes Earth's surface at a variety of incidence angles, footprint size varies; the nominal size is about 43 km. From this point forward we will refer to non-overlapping circles of diameter 43 km centered on SMOS grid points as SMOS "pixels." Iowa has 99 counties, or political units just below the state level, and the average size of an Iowa county is approximately the same as one SMOS pixel. Hence there are roughly 100 unique SMOS pixels in the state.

We found 30 SMOS pixels in Iowa in which the percentage of land devoted to annual crops was greater than 75% and as large as 85%. These cropped areas are planted almost exclusively in maize and soybean. All 30 of these pixels fall within the northwest half of the state, and all but 6 reside within the northwest quarter. We chose to investigate the behavior of τ in all 30 pixels, and to specifically highlight the behavior of τ in 5 of the 30 pixels which together represent the spatial diversity of the 30 pixels. The locations of these highlighted pixels are shown in Fig. 2. The first (Pixel 1) lies the farthest north and west. Pixel 2 is the farthest north and east. Pixel 4 is the eastern-most pixel and Pixel 5 is the farthest south and west. Pixel 3 is roughly equidistant from the other four. The percentage of each of the five pixels that is covered with "nominal" or "low" amounts of vegetation for which SMOS attempts soil moisture retrieval, and the fractions of row cropped land planted to maize in each pixel from 2010 to 2013, are listed in Table 1.

2.1.1. Smoothing of SMOS optical thickness

SMOS optical thickness exhibits high-frequency noise (large variations on the order of a day). A representative example of τ data for a SMOS pixel in north-central Iowa is shown in Fig. 3. Vegetation biomass, especially at the satellite scale, should not vary disjointedly from one day to the next as is shown in this record. Variations of more than 30% in the value of τ within the month of August can be seen in Fig. 3. By this time of the growing season crops in Iowa have reached a stage of development (the grain-filling period) during which plants are gradually increasing their mass. Patton and Hornbuckle (2013) speculated that this high-frequency noise may be caused by low levels of radio

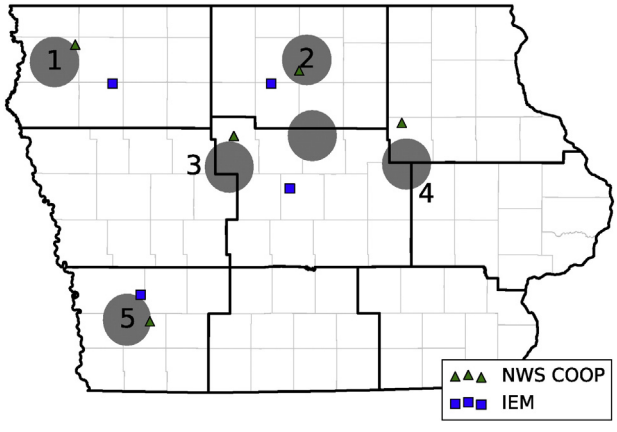

Fig. 2. The locations of the five highlighted SMOS pixels for which we examine the change in τ over time. The bold lines mark the border of the state of Iowa and the nine USDA Crop Reporting Districts within the state. The faint outlines are the 99 Iowa counties. Also shown are the locations of the NWS COOP and IEM Soil Moisture Network stations at which meteorological data were recorded. The unnumbered SMOS pixel covers the watershed of the South Fork Iowa River. Data for this pixel are used in Fig. 13.

Please cite this article as: Hornbuckle, B.K., et al., SMOS optical thickness changes in response to the growth and development of crops, crop management, and weather, *Remote Sensing of Environment* (2016), http://dx.doi.org/10.1016/j.rse.2016.02.043

Table 1
Land cover characteristics for each of the five numbered SMOS pixels shown in Fig. 2 along with their DGG identifiers. The "nominal fraction" is the fraction of each pixel covered with "nominal" vegetation or vegetation whose water column density is low enough for SMOS to attempt a soil moisture retrieval. The final five columns consider the cropped land in each pixel planted in either maize or soybean, and lists the fraction of this land area that was planted in maize according to USDA data.

Pixel	DGG	Nominal fraction	Mean maize fraction	2010	2011	2012	2013
1	194,406	0.9812	0.628	0.603	0.635	0.630	0.644
2	197,495	0.9469	0.640	0.627	0.656	0.653	0.625
3	200,052	0.8921	0.602	0.586	0.600	0.631	0.591
4	202,112	0.8556	0.587	0.569	0.605	0.590	0.584
5	203,632	0.9973	0.538	0.518	0.545	0.545	0.544

frequency interference (RFI), anthropogenic emission of microwave radiation from weather radars and other sources.

On the other hand, there are diurnal changes in the water content of crops that may be significant at the satellite scale. The water potential of plant tissue, and consequently plant water content, changes over the course of a day as a result of transpiration, the movement of water from the soil, into plant roots, through a plant's vascular system, and eventually out of the stomata in its leaves (Slatyer, 1967). Hunt, Niemeier, da Cunha, and Kruger (2011) observed this diurnal change through the analysis of cellular signals propagating through a field of maize. They found that signal strength was inversely proportional to vegetation water content. A clear diurnal pattern, with vegetation water content being largest at night and lowest during daylight hours, appeared when the data was detrended to account for the seasonal change.

Rowlandson, Hornbuckle, Bramer, Patton, and Logson (2012) found that during the growing season in the Corn Belt, SMOS soil moisture retrieved at 6 AM solar time was wetter than soil moisture retrieved 12 h earlier for periods when such measurements were available due to the characteristics of the SMOS satellite's orbit. They only considered 12-hour periods when no precipitation fell. They compared these differences in SMOS soil moisture to natural changes in soil moisture that occur overnight. They found that the changes observed by SMOS were significantly larger than changes observed by in situ soil moisture sensors and predicted by an agro-ecosystem model. They concluded that these changes in SMOS soil moisture were likely caused by an increase in vegetation water content overnight that SMOS wrongly interpreted as a change in soil moisture.

While significant diurnal variations in τ at the satellite scale may exist, we analyze in this paper the seasonal change in τ. Therefore, our use of a smoothing method that removes natural and possibly artificial high-frequency variations in τ that occur over time periods of less than a week is appropriate. Initially we used a simple moving-average method in which the mean value of sets of τ values centered over each point in time are analyzed (Patton & Hornbuckle, 2013). In this investigation we use functional data analysis (FDA). An FDA method assumes that the data is fundamentally smooth and continuous and can therefore be represented by a smooth and continuous function or superposition of functions.

We used the R programming environment FDA package (Ramsay, Wickham, Graves, & Hooker, 2013) to smooth the τ data using a Fourier basis (sines and cosines) with a roughness penalty Λ that minimizes the magnitude of the second derivative of the fit function according to the magnitude of Λ. We allowed the periods of the sine and cosine functions to vary between 12 h and 365 days. We chose to use $\Lambda = 10^4$ since this value allowed the fitting function to not react strongly to the high frequency noise, as was the case for $\Lambda = 10^3$, and to not greatly reduce the amplitude of the τ signal, as was the case for $\Lambda = 10^5$. Raw τ data, τ smoothed using a 21-day moving average, and τ smoothed using FDA are shown in Fig. 3. Our FDA method produced a τ signal similar to one produced using a moving average. Both effectively eliminate the high-frequency noise that is observed in the raw τ data.

For "well-behaved" data sets there are ways to determine Λ analytically. However, SMOS τ is not well-behaved. The noise has a period of roughly 18 days and the covariance of the noise remains high, even after 90 days (Patton, 2014). The exact repeat cycle of a SMOS swath is 149 days. While 149 is prime, 18 is a factor of 144, so it is possible that the noise is a function of the position of a pixel within the satellite's swath. This position within the swath determines how many and which incidence angles are available to make retrievals. It is also known that there are biases in observed brightness temperature within the swath. More investigation is needed to determine the cause of this high frequency noise.

The resulting function for τ in Fig. 3 has a distinct peak in August, and in this example for a pixel in Kossuth County (the largest county in the North Central USDA Crop Reporting District in Fig. 2), another peak in early November. Troughs occur in early June and at the beginning of October. The two troughs and the peak in August can be easily explained by the growth cycle of annual crops. In Iowa, crops are typically planted in late April or May, increase in water column density until sometime in August, begin to senesce and dry out in September, and are harvested in late September or October.

The second peak also has a physical explanation. SMOS τ is not only affected by vegetation: changes in soil surface roughness cause SMOS τ to change because soil surface roughness and vegetation affect terrestrial microwave brightness temperature in similar ways (Njoku & Chan, 2006; Patton & Hornbuckle, 2013). Since the SMOS retrieval algorithm assumes that soil surface roughness is constant, temporal changes in the soil surface roughness manifest themselves as changes in τ. The second peak in τ in Fig. 3 can thus be explained by an increase in soil surface roughness caused by management (tillage) after crops are harvested in late September and October (Patton & Hornbuckle, 2013).

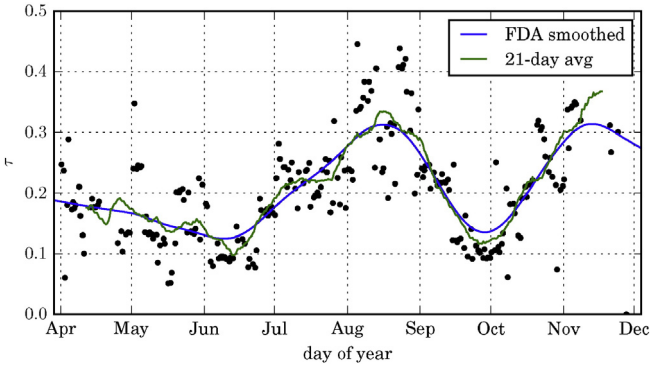

Fig. 3. Raw SMOS optical thickness τ, τ smoothed using a 21-day averaging window, and τ smoothed using Fourier-based functional data analysis (FDA). Data is for a pixel in Kossuth County, IA, in 2010. Kossuth County is the largest county within the north-central Crop Reporting District in Fig. 2.

2.2. Crop progress

We used USDA NASS data to determine the date of management activities such as planting and harvest and the dates at which crops had reached specific stages of crop development. The USDA posts weekly National Crop Progress and Condition reports as well as data for Crop Reporting Districts within individual states at http://www.nass.usda.gov (accessed December 2015). Estimates of the timing of two management activities (planting and harvest) and seven different developmental stages for maize (emergence, tassle, silk, milk, dough, dent, and maturity) are reported. Two management activities (planting and harvest) and five different developmental stages are reported for soybean (emergence, bloom, setting pods, leaves color, and dropping leaves). An example of this data is shown in Fig. 4 which illustrates the timing of planting,

Please cite this article as: Hornbuckle, B.K., et al., SMOS optical thickness changes in response to the growth and development of crops, crop management, and weather, *Remote Sensing of Environment* (2016), http://dx.doi.org/10.1016/j.rse.2016.02.043

ARTICLE IN PRESS

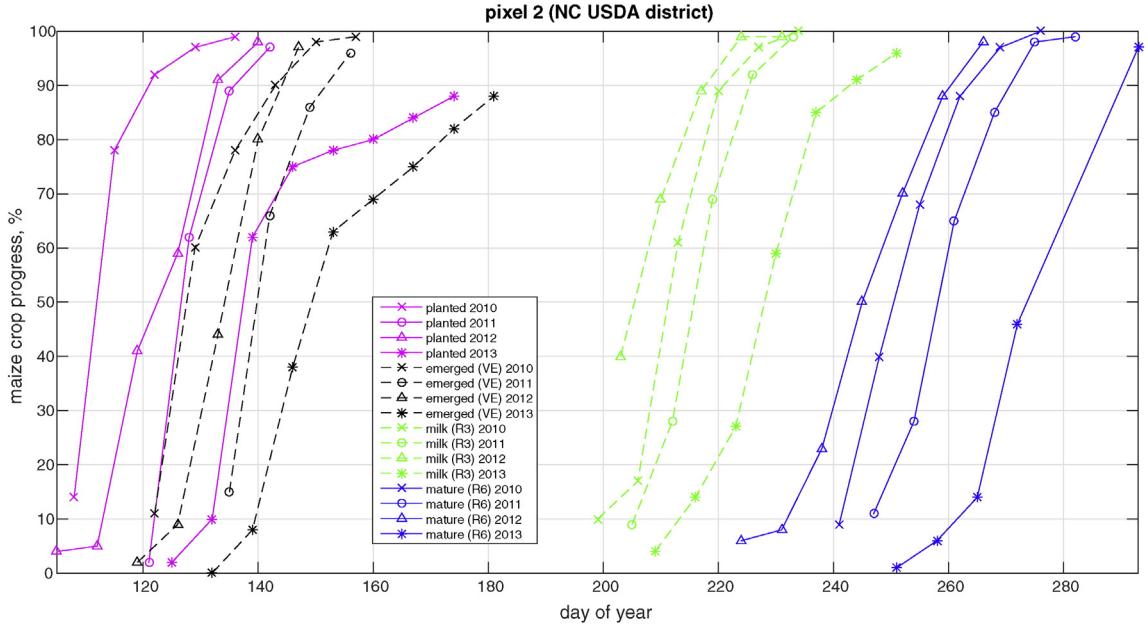

Fig. 4. Crop progress information for maize in the north-central district of Iowa (Fig. 2) for 2010–2013.

emergence, the third reproductive stage, and harvest for maize over the four-year period of our investigation.

The data are collected via approximately 4000 visual surveys conducted by people who are in frequent contact with farmers. The surveyors are normally agricultural extension agents (liaisons between state land-grant universities and the agricultural community) or USDA employees. There is at least one survey completed in every county. Since there are 9 USDA Crop Reporting Districts in Iowa, the smallest district contains 9 counties, and there are 99 counties in Iowa, each data point represents information from a minimum of approximately 10 surveys. Data are reviewed for reasonableness and consistency and are weighted according to the land area of each county devoted to crops. Since this data is given in terms of percentages of crops that have reached specific developmental stages, we used the date on which 50% of management activities had been completed or 50% of the crops had reached the relevant developmental stage in our analysis. As indicated in Fig. 2, Pixels 1, 2, and 5 reside wholly within separate Crop Reporting Districts. In order to determine the timing of crop management and development events in the other two pixels, we weighted the dates according to the fractions of Pixels 3 and 4 that lay within each Crop Reporting District.

2.3. Meteorology

The meteorological data used in our analysis were acquired from three different sources. Daily maximum and minimum air temperature and daily precipitation were provided by the National Weather Service Cooperative Observer Program (NWS COOP) via the Iowa Environmental Mesonet (IEM). Gaps in the data were filled with estimates made by the Iowa State Climatologist or the National Centers for Environmental Information. NWS COOP stations are spaced roughly every 40 km throughout the U.S. We made an effort to select weather stations located within each of the 30 SMOS pixels. When this was not possible, the station nearest to each pixel was used. The locations of the NWS COOP sites for each of the five highlighted pixels are listed in Table 2 and shown in Fig. 2. We also used daily precipitation data from Daymet (Thornton, Running, & White, 1997; Thornton et al., 2014). The nature of Daymet data allowed us to use estimated precipitation at the geographic center of each pixel.

Solar radiation as well as additional air temperature data relevant to the five highlighted pixels were acquired from the IEM Soil Moisture Network (http://mesonet.agron.iastate.edu/agclimate/, accessed December 2015). Missing data were gap-filled using linear interpolation and/or spatial averaging of adjacent weather stations. Gap-filled data accounted for less than 2% of the total data set. The locations of the IEM Soil Moisture Network sites for each pixel are listed in Table 3 and shown in Fig. 2. The Sutherland station was replaced by Calumet in 2013. Because of the limited number of sites, the sites do not match the five SMOS pixels in Fig. 2 as well as the NWS COOP sites and the same data were used for Pixels 3 and 4. However, the IEM Soil Moisture Network provides another set of independent information collected directly in agricultural fields (as opposed to cities where many NWS COOP volunteers reside and observe weather conditions) that strengthen our conclusions.

2.4. Crop biomass

In order to characterize how the water column density of maize and soybean change over time, we used in situ measurements from fields near Mead, NE, where maize and soybean were grown at three different sites from 2003 until 2011. The crops were irrigated. Planting dates were recorded, and about every 10 days destructive samples of crop biomass were obtained (individual plants were cut at the soil surface and were massed, dried, and massed again). The stage of development was also recorded. The samples were used to calculate the column density of vegetation, defined as the mass of vegetation per ground area. Both fresh, M_f, and dry, M_d, column densities were measured directly (kg m^{-2}); M_d after drying the fresh vegetation for several days. We found the water column density of vegetation, M_w, the mass of water contained within vegetation tissue per ground area, sometimes referred

Table 2
Locations of National Weather Service Cooperative Observer Program (NWS COOP) stations at which data on air temperature and precipitation were acquired for each SMOS pixel shown in Fig. 2.

Pixel	Name	Latitude	Longitude
1	Sheldon	43.2° N	95.9° W
2	IA NC Climate Division	43.0° N	93.5° W
3	Fort Dodge	42.5° N	94.2° W
4	Waterloo	42.6° N	92.4° W
5	IA SW Climate Division	41.1° N	95.1° W

Please cite this article as: Hornbuckle, B.K., et al., SMOS optical thickness changes in response to the growth and development of crops, crop management, and weather, *Remote Sensing of Environment* (2016), http://dx.doi.org/10.1016/j.rse.2016.02.043

Table 3
Locations of Iowa Environmental Mesonet (IEM) Soil Moisture Network stations at which data on solar radiation and air temperature were acquired for each SMOS pixel shown in Fig. 2.

Pixel	Name	Latitude	Longitude
1 (2010–2012)	Sutherland	42.9° N	95.5° W
1 (2013)	Calumet	42.9° N	95.5° W
2	Kanawha	42.9° N	93.8° W
3 & 4	Gilbert	42.1° N	93.6° W
5	Lewis	41.3° N	95.2° W

to as the vegetation water content or VWC, using the relationship $M_f = M_w + M_d$.

3. Theory

3.1. Optical thickness

Within a medium such as a vegetation canopy, the incremental change in brightness temperature at each point is the sum of three effects (e.g., Ulaby, Moore, & Fung, 1981):

$$dT_B(\hat{s}) = -\kappa_e T_B(\hat{s})ds + \kappa_a T\,ds + \frac{\kappa_s}{4\pi}\int_{4\pi}\psi(\hat{s},\hat{s}')T_B(\hat{s}')d\Omega'\,ds. \quad (1)$$

where ds is an incremental distance and $d\Omega$ is an incremental solid angle. First, rays of radiation (traveling in some specific direction denoted by $\hat{s}$) are attenuated in proportion to the medium's extinction coefficient, κ_e. Extinction is due to both absorption (denoted by κ_a, the volume absorption coefficient) and scattering (denoted by κ_s, the volume scattering coefficient) such that $\kappa_e = \kappa_a + \kappa_s$. Second, the medium emits according to its temperature, T, in order to maintain thermodynamic equilibrium. Finally, radiation from all other directions $\hat{s}'$ can potentially be scattered into the $\hat{s}$ direction according to the function $\psi(\hat{s},\hat{s}')$.

The SMOS retrieval algorithm employs what is commonly called the $\tau-\omega$ model (Kerr et al., 2011, 2012; Wigneron et al., 2007) to account for the effect of soil moisture and vegetation on the brightness temperature observed by the L-band radiometer onboard the SMOS satellite. This model is a zero-order solution of Eq. (1) that neglects scattering of radiation into the beam (the third term in Eq. (1)) and enforces boundary conditions appropriate for a uniform layer of vegetation with diffuse boundaries over a soil surface. The model can be written

$$\begin{aligned} T_{B,p} = {} & T_{soil}(1-R_{soil,p})e^{-\tau_p/\cos\theta} \\ & + (1-\omega_p)T_{veg}\left(1-e^{-\tau_p/\cos\theta}\right) \\ & + (1-\omega_p)T_{veg}\left(1-e^{-\tau_p/\cos\theta}\right)R_{soil,p}\,e^{-\tau_p/\cos\theta}. \end{aligned} \quad (2)$$

In Eq. (2): $T_{B,p}$ is the p-polarized (h = horizontally polarized and v = vertically polarized) brightness temperature; T_{soil} is the effective temperature of the soil; $R_{soil,p}$ is the soil surface reflectivity; τ_p is the vegetation optical thickness; θ is the incidence angle; ω_p is the single-scattering albedo of the vegetation canopy; and T_{veg} is the effective temperature of the vegetation. At low microwave frequencies $T_{B,p}$ is sensitive to soil moisture since $R_{soil,p}$ in Eq. (2) is a strong, nearly linear function of the volumetric water content of soil. The three terms of Eq. (2) represent the three ways in which vegetation affects $T_{B,p}$: emission from the soil is attenuated as it passes through the vegetation canopy; the vegetation self-emits; and emission from the vegetation initially directed toward the ground is scattered by the soil surface and attenuated as it passes back through the vegetation canopy.

It is important to note a few details. First, Eq. (2) should only be used when κ_s is small enough relative to κ_a that the third term of Eq. (1) can be neglected. This is only appropriate when scattering within the canopy is not significant such as when the components (leaves, stems, fruit) of the canopy are small when compared to λ. The ω_p parameter in Eq. (2) represents the relative importance of scattering within the canopy such that

$$\omega_p = \frac{\kappa_{s,p}}{\kappa_{e,p}} = \frac{\kappa_{s,p}}{\kappa_{a,p}+\kappa_{s,p}}. \quad (3)$$

Therefore it must be small ($\omega_p << 1$) for Eq. (2) to be physically consistent with Eq. (1). This condition is likely to be satisfied at L-band for both maize (Hornbuckle et al., 2003) and soybean. The SMOS retrieval algorithm currently uses $\omega_p = 0$ for nominal vegetation.

Second, $\tau_p = \kappa_{e,p} z_{veg}$ where z_{veg} is the height (vertical thickness) of the vegetation canopy. In the SMOS retrieval algorithm it is further parameterized as

$$\tau_p = \tau_{NAD} f(\theta,p) \quad (4)$$

where τ_{NAD} is the optical thickness at nadir ($\theta = 0^{\circ}$) and $f(\theta,p)$ represents a function of θ and p that can account for anisotropy in the vegetation canopy. Currently $f(\theta,p) = 1$ is used for all types of vegetation and τ_{NAD} is assumed to be independent of polarization. Furthermore, it has been shown for many types of vegetation (including maize and soybean) that τ_{NAD} is directly proportional to M_w (Jackson & Schmugge, 1991).

$$\tau_{NAD} = b M_w \quad (5)$$

The proportionality constant is called the "b parameter" and is in reality a function of frequency, polarization, and the way in which water is distributed in stems and leaves (which is related to the type of vegetation). The b parameter for crops should be allowed to change over time as a function of crop development but it is normally kept constant. The model in Eq. (5) is consistent with the fact that $\kappa_{e,p} \approx \kappa_{a,p}$ when $\omega_p << 1$, and $\kappa_{a,p} = 2k_o \mathrm{Im}\{n_{veg}\}$ where $k_o = 2\pi/\lambda$ and n_{veg} is an effective index of refraction for a vegetation canopy, which would be dominated by the refractive index of water (Ulaby et al., 1981).

Third, soil surface roughness (mm-scale variations in the height of the soil surface) has a strong effect on $R_{soil,p}$ (Choudhury, Schmugge, Chang, & Newton, 1979). The SMOS retrieval algorithm uses the general model

$$R_{soil,p} = \left[(1-Q)R_p + Q R_q\right]e^{-H\cos^{N_p}(\theta)} \quad (6)$$

where: R_p is the reflectivity of a specular soil surface; q is the opposite polarization as p; the Q parameter allows for polarization mixing; H is a function of the root-mean-square height of the soil surface and possibly soil moisture (Wigneron, Laguerre, & Kerr, 2001); and N_p allows for dependence on θ. Currently values of $Q = 0$, $N_v = 0$, and $N_h = 2$ are used and Eq. (6) can be written as

$$R_{soil,p} = R_p\,e^{-h_p} \quad (7)$$

where h_p represents the effect of soil surface roughness which SMOS currently assumes depends on θ but does not change with time. Patton & Hornbuckle (2013) showed that when Eq. (7) is used in Eq. (2)

$$\Delta h_p = \frac{2}{\cos^{1+N_p}(\theta)}\Delta\tau_{NAD} \quad (8)$$

which means that changes in soil surface roughness, Δh_p, have a similar effect on $T_{B,p}$ as changes in τ_{NAD}, $\Delta\tau_{NAD}$. The consequence is that because h_p is currently not a function of time in the SMOS retrieval algorithm, actual changes in soil surface roughness (e.g., caused by tillage) result in changes in τ_{NAD}.

The SMOS mission retrieves soil moisture and τ_{NAD} by minimizing a cost function, which is essentially the difference between: $T_{B,p}$ predicted by Eq. (2) using auxiliary information; and observed $T_{B,p}$ (Kerr et al., 2011). The unique design of the SMOS instrument produces a large

Please cite this article as: Hornbuckle, B.K., et al., SMOS optical thickness changes in response to the growth and development of crops, crop management, and weather, *Remote Sensing of Environment* (2016), http://dx.doi.org/10.1016/j.rse.2016.02.043

number of observations of $T_{B,p}$ as a function of θ for each pixel which results in a higher level of confidence in retrieved soil moisture and τ_{NAD}. The SMOS Level 2 soil moisture processor has been tuned to give optimal soil moisture retrievals. However, future versions of the processor are expected to address the effect of temporal changes in soil surface roughness and potentially use specific values of ω_p and $f(\theta,p)$ for different types of vegetation.

It is readily apparent from Eq. (5) that since a large percentage of vegetation is water, τ_{NAD} increases as the amount of vegetation increases, as long as the distribution of water in the vegetation (as represented by b in Eq. (5)) does not change significantly. For simplicity, we use the symbol τ and the terminology "optical thickness" to refer to τ_{NAD}, the nadir optical thickness, the quantity that is actually retrieved by the SMOS algorithm. It is also imperative to keep in mind that because of the assumptions made by the retrieval algorithm, changes in τ represent both changes in the amount of vegetation and changes in the roughness of the soil surface, and, as found by Schlenz et al. (2012), possibly changes in soil moisture.

3.2. Crop development

Maize and soybean are annual crops and hence the mass of individual plants changes significantly over the growing season. Each progress through vegetative and reproductive stages of development (Abendroth, Elmore, Boyer, & Marlay, 2011; Pedersen, 2009). During the vegetative stages plant mass changes rapidly as new leaves appear and the stem increases in size. The first vegetative stage is emergence (VE) which occurs when a plant first protrudes from the soil. Subsequent vegetative stages correspond to the number of leaves (compound leaves for soybean) present: there is one leaf at V1; three leaves at V3; etc. For maize, there could be 17 to 22 vegetative stages before a tassel is visible, at which time the plant has reached VT (vegetative stage, tassel) and is now ready to begin the reproductive stages. For soybean, the vegetative and reproductive stages overlap, with the reproductive stage starting approximately at V8 while the plant eventually reaches V20.

Once a maize plant reaches the reproductive stages, its focus is on the development of the ear. A maize plant first produces silks which transfer pollen produced by tassels to each individual kernel on the ear (R1). After the kernels are fertilized they grow in size and the plant progresses through blister (R2), milk (R3), dough (R4), dent (R5), and full maturity (R6). Stages R2 through R5 describe the appearance of the kernels as they accumulate dry matter and decrease in moisture content. At R6 the plant has reached full maturity and no longer adds dry matter to the ear. A soybean plant progresses through similar reproductive stages. A senescence period during which annual plants cease photosynthesis, relocate nutrients from leaves and stems to reproductive organs, and rapidly decrease in water content overlaps with the reproductive stages.

Crops progress through developmental stages according to the temperature of their environment. The coldest temperature at which development occurs is called the base temperature, T_{base}. Through experimentation T_{base} for maize has been found to be about 10 °C (Abendroth et al., 2011). Above T_{base} maize development is directly proportional to temperature, up to a temperature $T_{ceiling}$ of about 30 °C. The amount of time that a maize plant accumulates above T_{base} and below $T_{ceiling}$ multiplied by the temperature above T_{base} is called thermal time (e.g., Campbell & Norman, 1998). The progression of the stages of development for a maize plant can be accurately predicted through the calculation of thermal time. Typically thermal time for maize is given in units of °C day and called growing degree days (GDD). The amount of GDD accumulated on a single day are normally calculated with sufficient accuracy as follows:

$$\mathrm{GDD} = \frac{T_{high} + T_{low}}{2} - T_{base} \tag{9}$$

where T_{high} and T_{low} are the daily high and low air temperature. Specific amounts of GDD accumulated over a number of days are needed for a maize plant to progress from one developmental stage to another. For example, emergence requires about 60 °C day. The developmental process for soybean is more complex than maize. In addition to GDD, soybean plants are sensitive to the period of sunlight (photoperiod) (Pedersen, 2009).

3.3. Crop growth

Monteith and Moss (1977) observed for several different crops that M_d is directly proportional to the amount of accumulated solar radiation intercepted by a green vegetation canopy such that

$$M_d \propto e f_S S \tag{10}$$

where f_S is the fraction of incident solar radiation S intercepted by the canopy and e is often called the radiation use efficiency (RUE) (Singer, Meek, Sauer, Prueger, & Hatfield, 2011) or light use efficiency (LUE) (Anderson, Norman, Meyers, & Diak, 2000). In reality, the amount of absorbed photosynthetically-active radiation (PAR) determines how much photosynthesis occurs and hence how much carbon a crop assimilates (and M_d increases), but PAR is essentially directly proportional to S (Campbell & Norman, 1998).

4. Calculation

We used the in situ crop data described in Section 2.4 to determine how the M_w of maize and soybean crops change over a typical growing season since changes in M_w directly affect τ according to Eq. (5). Fig. 5 displays what we found. The vertical axis of Fig. 5 is the column density (kg m^{-2}, measured using destructive sampling) of either water contained within the crop (M_w) or the dry column density ($M_d = M_f$–M_w). The black symbols are for maize (circles for maize M_w, stars for maize M_d) and the red symbols are for soybean (squares for soybean M_w, hexagrams for soybean M_d). The horizontal axis of Fig. 5 is time over a growing season in terms of GDD ($T_{base} = 10$°C) calculated using Eq. (9). We started this time reference at GDD = 0 when the maize crop was planted each year. Air temperature for the calculation of GDD was obtained from an NWS COOP station nearby. Note that this data consists of all of the measurements made in three different fields (two maize and one soybean) over the nine-year period described in Section 2.4.

As expected, M_d for both crops steadily increase or remain constant over time up until harvest at the end of the growing season as they accumulate dry matter as described by Eq. (10). In contrast, M_w for both maize and soybean rises and then falls, with a peak roughly in the middle of the period of the maize life cycle and about three-fourths of the way through the life cycle of soybean. Since the 30 SMOS pixels we investigated in Iowa contain both maize and soybean, we estimated what the total M_w of a hypothetical SMOS pixel might be using the average fraction of cropland planted in maize over the four-year period for the five pixels in Fig. 2, 0.599, calculated using the information in Table 1. This estimate of the total M_w that would be expected to occur within a typical SMOS pixel in Iowa is the solid line in Fig. 5.

Note that total pixel M_w peaks at close to 1000 °C day. Changing the fraction of corn (and consequently soybean) to a value other than the four-year mean value (as shown in Table 1) to match a specific year will only slightly increase or decrease the magnitude of the solid line in Fig. 5. It will not change when this line reaches its maximum value, at roughly 1000 °C day.

5. Results

An example of the temporal variation of SMOS τ (smoothed using the procedure described in Section 2.1.1) for the 2010, 2011, 2012,

Please cite this article as: Hornbuckle, B.K., et al., SMOS optical thickness changes in response to the growth and development of crops, crop management, and weather, *Remote Sensing of Environment* (2016), http://dx.doi.org/10.1016/j.rse.2016.02.043

ARTICLE IN PRESS

and 2013 growing seasons is shown in Fig. 6. This example is for Pixel 2 in Fig. 2. SMOS τ reached its peak value earliest in 2012 and latest in 2013. Accumulated meteorological data for each pixel and for each year from April 1 to the end of the year are given in Table 4. Note that Pixel 2 accumulated the most GDD in 2012 and the least in 2013. Furthermore, the order of accumulated GDD (2012, 2010, 2011, 2013) exactly matches the timing of the peak values of τ. We found this pattern also to be true for Pixels 1 and 4. The value of τ in Pixels 3 and 5 also peaked the earliest in 2012, the year in which all pixels accumulated the most GDD. Besides differences in timing among the four years, there are also significant differences in the peak value of τ.

We tested the two hypotheses in Section 1 using the data described in Section 2. For each test, we computed Pearson correlation coefficients R and p-values with MATLAB software version R2013a. The correlation coefficient R indicates whether a linear relationship exists between two phenomena. Its value ranges between -1 and 1 (values that imply perfect negative and positive linear relationships, respectively) and a value of $R = 0$ implies that no linear relationship exists. The square of R, or R^2, is called the coefficient of determination and is an estimate of the fraction of the variance in the dependent variable in a linear relationship that can be explained by the independent variable. One interpretation of the p-value is the probability that the null hypothesis is true, or in other words, that there is no relationship between two phenomena. Another interpretation of the p-value is the probability of getting a correlation as large as the observed correlation R by random chance, if the true value of R is zero.

5.1. Hypothesis 1: timing

To test our first hypothesis regarding the timing of the maximum value of SMOS τ, we used the vegetation data in Section 2.4 to determine at what developmental crop stage we expected pixel M_w, and therefore τ, to be the largest. Since maize accounted for the majority (59.9% on average) of the cropped area in the pixels that we examined, maize M_w is much larger than soybean, and consequently the overall M_w of a hypothetical SMOS pixel (the solid line in Fig. 5) peaks when maize M_w peaks, we searched for the developmental stage at which maize M_w was largest. Of the 20 sets of maize data, one indicated that maize M_w was largest at R1 (silk), 8 indicated that M_w was largest at R2 (blister), 5 at R3 (milk), 3 at R4 (dough), and 3 at R5 (dent). Not all stages were sampled in each set, so it is not surprising that the largest values of M_w were observed at a variety of reproductive stages. The data appear to indicate that maximum maize M_w occurs at roughly R2 to R3.

Since the R2 stage is not reported by the USDA, we examined the relationship between the day of year of maximum τ and the day of year at which 50% of the maize crop within the relevant Crop Reporting District for each of the five SMOS pixels had reached R3. The result is shown in Fig. 7. The relationship has a high value of $R = 0.81$ and a low p-value of 1.5×10^{-5}. The values of these two statistical descriptors are impressive considering the nature of the USDA survey data and the size of SMOS pixels relative to the size of the Crop Reporting Districts.

To further test our first hypothesis, we determined when 1000 °C day of GDD had been accumulated from the time of maize planting, since the data in Fig. 5 indicate that when this amount of thermal time has been accumulated, M_w for a hypothetical mixed pixel containing both maize and soybean would be largest. We compared the day of year at which 1000 °C day had been accumulated to the day of year of the maximum value of SMOS τ. We used the date on which 50% of maize had been planted in the respective Crop Reporting District as the date of maize planting for each pixel. The results are shown in Figs. 8 and 9. In Fig. 8, we calculated GDD using the NWS COOP data, and in Fig. 9 we used air temperature from the IEM Soil Moisture Network.

The values of R and p for each figure are again impressive considering the nature of the data: $R = 0.74$ and $p = 1.8 \times 10^{-4}$ when using NWS COOP data; and $R = 0.78$ and $p = 4.3 \times 10^{-5}$ when using data from the IEM Soil Moisture network. Both figures appear to indicate that SMOS τ peaks at close to 1000 °C day or perhaps slightly later. Pixels 3–5 in Fig. 8 each exhibit the following pattern. Without exception, if the day of year of maximum τ was later in one year than another year, then the day on which 1000 °C day had been accumulated was later than (or equal to in the case of 2010 and 2011 for Pixel 4) the day on which 1000 °C day had been accumulated for the other year. Among all five of the pixels, only two data points, for Pixel 1 in 2013 and Pixel 2 in 2011, do not follow this pattern. For Fig. 9 there is only one outlier, in 2011 for Pixel 1. We have no explanations for these outliers: all are wholly contained within their respective Crop Reporting District (the northwest district for Pixel 1 and the north-central for Pixel 2); each pixel has a high nominal fraction according to Table 1; and our procedure for verifying the quality of the NWS COOP and IEM data did not indicate any unusual behavior.

Data similar to Figs. 8 and 9 but for all 30 SMOS pixels in Iowa with greater than 75% coverage by maize and soybean is shown in Fig. 10. The value of $R = 0.73$ is similar to what we found for the five representative pixels using both the NWS COOP and IEM data, and $p = 2.6 \times 10^{-21}$. Note that the extreme years of 2012 (highest accumulation of GDD)

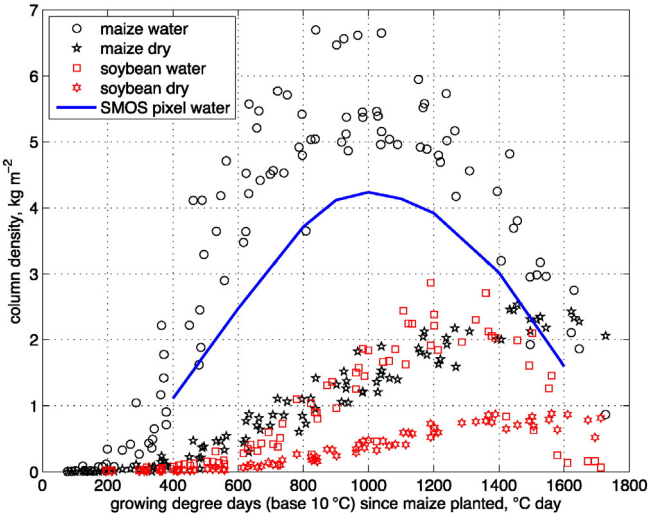

Fig. 5. Water column density, M_w, and dry column density, M_d, of irrigated maize and soybean as a function of growing degree days since maize was planted. The data was collected in agricultural fields near Mead, NE. Both the maize and soybean were irrigated to ensure that the plants always had adequate soil water. The solid line is an estimate of the resulting theoretical overall water column density of a hypothetical SMOS pixel with a corn fraction of 0.599, the average corn fraction across the four years and five pixels in Fig. 2 according to Table 1.

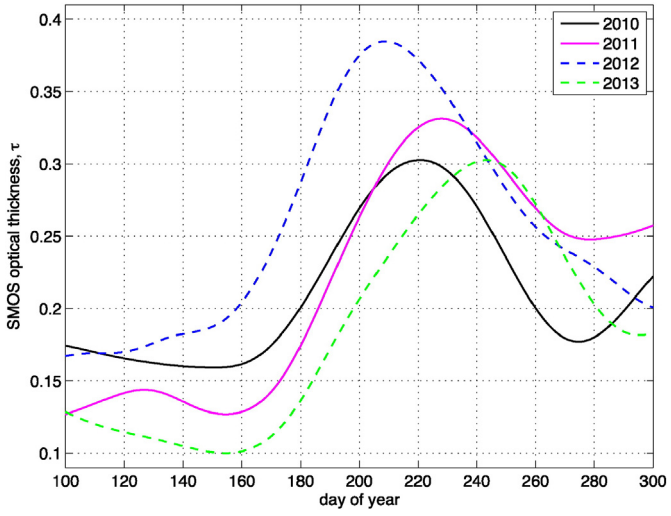

Fig. 6. Temporal variation of smoothed SMOS optical thickness, τ, from 2010 to 2013 for Pixel 2 in Fig. 2.

Please cite this article as: Hornbuckle, B.K., et al., SMOS optical thickness changes in response to the growth and development of crops, crop management, and weather, *Remote Sensing of Environment* (2016), http://dx.doi.org/10.1016/j.rse.2016.02.043

Table 4
Accumulation of meteorological variables beginning April 1 extending through end of year. For each combination of pixel and value, bold type indicates year of greatest accumulation and italicized type denotes year of lowest accumulation. Growing degree days (GDD) are calculated using air temperature from NWS COOP data, precipitation is from Daymet, and solar radiation is from the IEM Soil Moisture Network.

Pixel	Year	GDD (°C day)	Precip (mm)	Solar rad. (MJ m^{-2})
1	2010	1.53×10^3	**957.6**	4.15×10^3
	2011	1.43×10^3	476.7	*3.61×10^3*
	2012	**1.64×10^3**	*417.4*	3.81×10^3
	2013	*1.40×10^3*	629.6	**4.87×10^3**
2	2010	1.66×10^3	**891.3**	**4.21×10^3**
	2011	1.60×10^3	529.7	*3.55×10^3*
	2012	**1.77×10^3**	*426.5*	3.86×10^3
	2013	*1.55×10^3*	750.6	4.07×10^3
3	2010	1.61×10^3	**1120.0**	4.12×10^3
	2011	*1.48×10^3*	*511.7*	*3.41×10^3*
	2012	**1.67×10^3**	526.3	3.80×10^3
	2013	1.52×10^3	739.2	**4.22×10^3**
4	2010	1.75×10^3	**1130.0**	4.12×10^3
	2011	*1.63×10^3*	659.0	*3.41×10^3*
	2012	**1.81×10^3**	*517.2*	3.80×10^3
	2013	*1.63×10^3*	894.1	**4.22×10^3**
5	2010	1.95×10^3	**873.1**	**4.42×10^3**
	2011	1.91×10^3	799.8	*3.76×10^3*
	2012	**2.12×10^3**	*534.8*	4.23×10^3
	2013	*1.82×10^3*	709.5	4.21×10^3

and 2013 (lowest) according to Table 4 are clearly grouped. These results support our choice of using 5 pixels to represent the entire set of 30 pixels.

5.2. Hypothesis 2: magnitude

To test our second hypothesis regarding the increase in SMOS τ over the growing season, we plotted the increase in τ from maize emergence to the maximum value of τ, a quantity that we will refer to as $\Delta\tau_v$, versus the accumulated solar radiation over the same time period. Again, we used the date on which 50% of the maize crop had emerged in each pixel's Crop Reporting District as the date of maize emergence. The result is shown in Fig. 11. The value of $R = -0.38$ is low and the data are negatively correlated. We conclude that the amount of accumulated solar radiation is not what causes the value of $\Delta\tau_v$ to change from year to year.

We also investigated the relationship between $\Delta\tau_v$ and the fraction of cropland in each pixel planted in maize. We obtained values of $R = 0.40$ and $p = 0.083$ (not shown) which suggest that while maize M_w is larger than soybean, the presence of more maize may only explain a small portion of the differences in $\Delta\tau_v$ among the four years.

6. Discussion

Our first hypothesis regarding the timing of the maximum value of SMOS τ in the Corn Belt is supported by the data in Figs. 7, 8, 9, and 10. There are some additional interesting features in Fig. 10. The maximum value of τ for each of the 30 pixels was, in general, reached earliest in the 2012 season, followed by 2010, 2011, and then 2013. However, note that Fig. 1 indicates that each year's most intense periods of planting (the week during each year that the highest percentage of maize was planted) occurred first in 2010, two weeks earlier than in 2011, and three weeks earlier than in 2013. In 2012 there were two important planting periods, one occurring between the 2010 and 2011 periods, and the other after the 2011 period. Although planting occurred later in 2012 than in 2010 and 2011, the first 1000 °C day of GDD must have accumulated more rapidly in 2012 than in the other years, causing crops to develop at a faster rate and resulting in the earliest maximum value of τ. This conclusion is consistent with the data in Table 4 which indicate that 2012 was the warmest of the four years (each of the five highlighted pixels accumulated the most GDD in 2012).

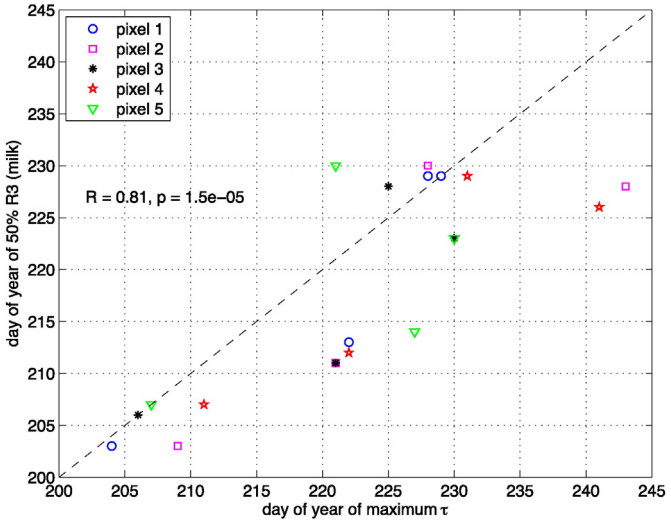

Fig. 7. The day of year at which 50% of maize had reached the R3 (milk) stage in each pixel's USDA Crop Reporting District versus the day of year the maximum value of SMOS τ was observed, for each of the five highlighted pixels and each year.

On the other hand, we did not find our second hypothesis to be true. The change in τ from maize emergence to its maximum value ranges from about $\Delta\tau_v = 0.13$ to 0.27 Np according to Fig. 11. Using Eq. (5), these changes in $\Delta\tau_v$ can be interpreted in terms of changes in M_w. Since the SMOS mission retrieves τ directly, there is no need to set a value for the b parameter. Another L-band satellite, NASA's Soil Moisture Active Passive (SMAP) mission (Entekhabi et al., 2010), assumes $b = 0.110$ for "croplands" (O'Neill, Chan, Njoku, Jackson, & Bindlish, 2015). Using $b = 0.110$, a $\Delta\tau_v$ of 0.13 to 0.27 Np would be equivalent to an increase in M_w of 1.2 to 2.5 kg m^{-2}. This is much less than what is indicated by Fig. 5, which shows an increase in pixel-scale M_w of about 4.0 kg m^{-2} over the growing season.

There are five things to take into account. First, we assume that the maximum value of M_w is correlated with the maximum value of M_d and therefore S according to Eq. (10). Second, despite the large fraction of maize and soybean in each of the five pixels, 15 to 25% of each pixel is some other type of landcover. In Iowa, the majority of this land area would be pasture (grass). For pasture we would expect smaller growing-season changes in τ. It is also possible that SMOS products could contain errors if significant urban areas or forests are present within a

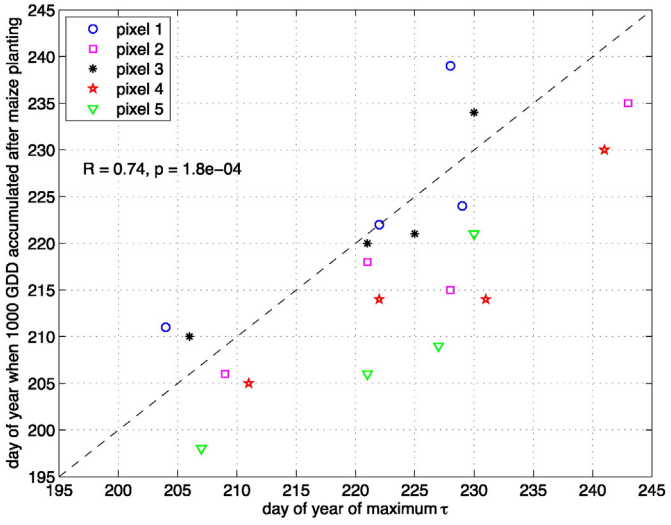

Fig. 8. The day of year at which 1000 °C day GDD were accumulated since the planting of maize according to NWS COOP air temperature data, versus the day of year the maximum value of SMOS τ was observed, for each of the five highlighted pixels and each year.

Please cite this article as: Hornbuckle, B.K., et al., SMOS optical thickness changes in response to the growth and development of crops, crop management, and weather, *Remote Sensing of Environment* (2016), http://dx.doi.org/10.1016/j.rse.2016.02.043

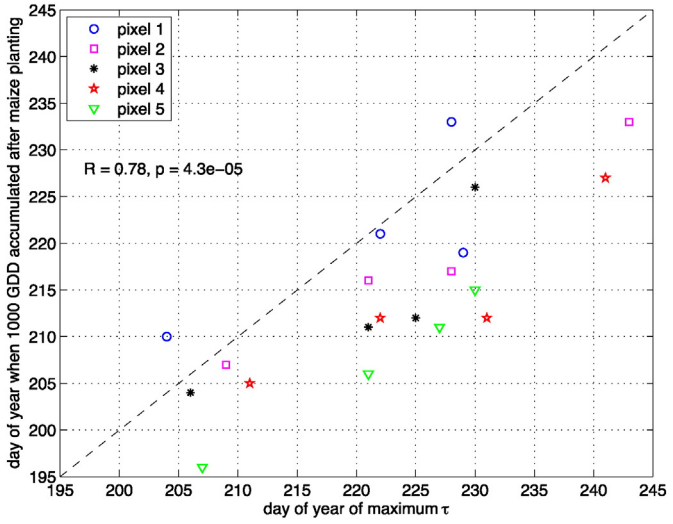

Fig. 9. The day of year at which 1000 °C day GDD were accumulated since the planting of maize according to IEM Soil Moisture Network air temperature data, versus the day of year the maximum value of SMOS τ was observed, for each of the five highlighted pixels and each year.

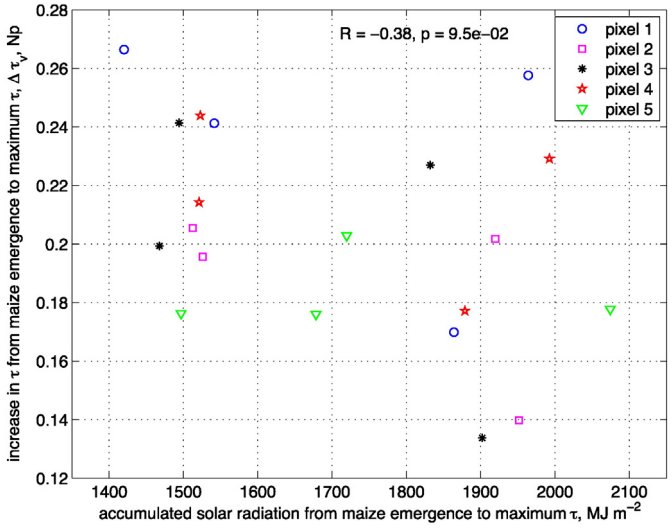

Fig. 11. The increase in SMOS τ from the time of maize emergence to the observed maximum value of τ, $\Delta\tau_v$, versus accumulated solar radiation (proportional to accumulated PAR) during the same time period.

pixel, since the products are only given for the portion of the pixel for which a successful retrieval is anticipated (the nominal fraction of the pixel, i.e. bare soil and "low" vegetation). This is done by modeling and subtracting out the contributions of urban areas and forests to the overall brightness temperature. However, Table 1 indicates the nominal fractions of the five representative pixels are high and therefore it is likely that the other 15 to 25% of each pixel would tend to reduce the value of $\Delta\tau_v$.

Third, since SMAP uses $\omega = 0.05$ (O'Neill et al., 2015), the appropriate value of b for SMOS, which assumes $\omega = 0$, would be slightly less than the SMAP value. This would increase the magnitude of the corresponding changes in M_w. Fourth, the data in Fig. 5 are for irrigated crops and therefore represent the maximum increase in M_w that would be observed. Irrigation is extremely rare in Iowa and hence crops may experience water stress at some point during the growing season which would stunt their growth and reduce $\Delta\tau_v$.

Finally, recall that changes in soil surface roughness are manifested as changes in SMOS τ. After tillage, soil surface roughness decreases exponentially in response to precipitation as raindrops hit and erode the soil surface (Zobeck & Onstad, 1987). According to Patton & Hornbuckle (2013), a decrease in SMOS τ of between 0.11 and 0.18 Np can occur simply due to rain that falls over the growing season: the value of the soil surface roughness of freshly tilled soil at the beginning of the growing season is greater than the value of soil surface roughness before harvest. Assuming $b = 0.110$, this is equivalent to a change in M_w of 1.0 to 1.6 kg m^{-2}. Adding this effective change in M_w caused by a decrease in soil surface roughness (and not by changes in vegetation) to the observed change in M_w derived from $\Delta\tau_v$ results in actual changes in M_w of between 2.2 to 4.1 kg m^{-2}, which encompasses the change in pixel-scale M_w indicated by Fig. 5.

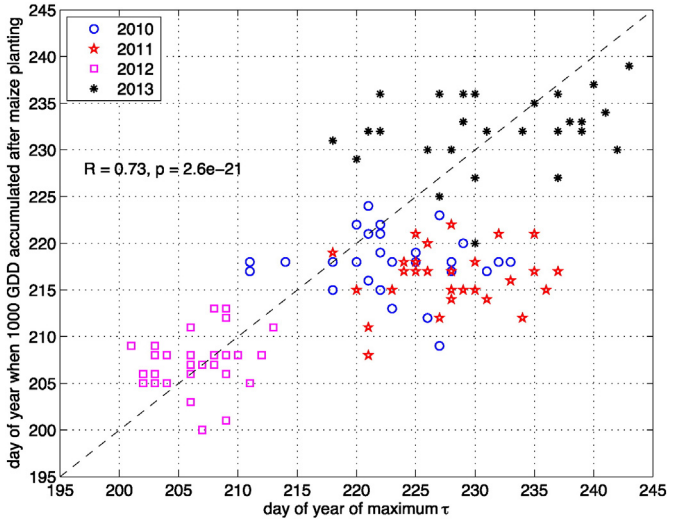

Fig. 10. The day of year at which 1000 °C day GDD were accumulated since the planting of maize according to NWS COOP air temperature data, versus the day of year the maximum value of SMOS τ was observed, for all 30 pixels in Iowa for which more than 75% of land area was devoted to maize and soybean, and each year.

6.1. Potential effect of precipitation on the magnitude of τ

Since precipitation decreases soil surface roughness and therefore SMOS τ, we investigated the possible effect of year-to-year variability in precipitation on the magnitude of τ by comparing $\Delta\tau_v$ with Daymet precipitation accumulated over the same time period. The results are shown in Fig. 12. The $R = -0.76$ and $p = 1.2 \times 10^{-4}$ values indicate a significant negative relationship between the two variables: smaller growing season increases in τ occurred in years in which more precipitation fell. On the other hand, similar changes in $\Delta\tau_v$ occur each year in Pixel 5. Comparable results were found using NWS COOP data ($R = -0.66$, $p = 1.5 \times 10^{-3}$).

We can think of two explanations. First, too much rainfall negatively affects crop growth. When soils are saturated, plant roots do not have adequate access to oxygen and respiration is impaired. Inadequate root growth can limit crops to soil water near the soil surface which can be depleted more readily than deeper soil moisture, leading to reduced plant growth. Excess water can also leach nitrate, which supplies nitrogen, an essential crop nutrient, out of the root zone which will result in reduced crop growth and hence a lower water column density (Connor, Loomis, & Cassman, 2011). But this does not explain why $\Delta\tau_v$ in Pixel 5 was the same in 2010 as it was in 2011 and 2012.

The other possibility is that the large amount of precipitation in 2010 (see Table 4) resulted in significantly different changes in soil surface roughness in 2010 as compared to the other three years. According to Eq. (8), smaller values of $\Delta\tau_v$ could result from: a larger decrease in soil surface roughness between crop emergence and the day at which the maximum value of τ was reached; or from less of an *increase* in soil surface roughness between crop emergence and the day at which the maximum value of τ was reached.

Please cite this article as: Hornbuckle, B.K., et al., SMOS optical thickness changes in response to the growth and development of crops, crop management, and weather, *Remote Sensing of Environment* (2016), http://dx.doi.org/10.1016/j.rse.2016.02.043

The total change in soil surface roughness will depend on three things: the types of management activities, such as tillage and fertilizer application, that occur before, during, and after crops are planted; the weather conditions that follow the planting of crops; and the timing of the weather conditions, since precipitation that precedes the point in time at which crops have grown sufficiently to shield the soil surface would result in larger reductions of the roughness of the soil surface. However, the anomalous behavior of Pixel 5 is perhaps a clue that management practices may also play a role. The topography of southwest Iowa is stronger than in the other regions of the state in which Pixels 1–4 reside. The greater the slope, the more soil is susceptible to erosion. It is desirable to keep soil in the field. Consequently, different management strategies that reduce the potential for soil erosion (e.g., reduced tillage, different methods of fertilizer application) and which result in less of a change in soil surface roughness between maize emergence and the maximum value of τ from year-to-year, regardless of weather conditions, may be practiced in Pixel 5.

Recall that Schlenz et al. (2012) found SMOS τ and SMOS soil moisture to be correlated. In theory, there should be little correlation between these two SMOS products in the Corn Belt: while soil is wet from the surface by precipitation, crop roots extend much farther below the emitting depth at L-band; and much of the soil water used by crops during the growing season originates from precipitation that occurs outside of the growing season. We examined SMOS θ_v and τ for a pixel in central Iowa that encompasses a large part of an in situ soil moisture network in the watershed of the South Fork Iowa River that has been established for SMAP validation. This SMOS pixel is one of three examined by Rondinelli et al. (2015). The correlation between SMOS soil moisture and τ is shown in Fig. 13 for the three years that the in situ soil moisture network has been in operation.

Rondinelli et al. (2015) found that SMOS soil moisture was positively correlated with the mean value of the 20 monitoring sites of the network at which soil moisture is measured with buried sensors at a depth of 5 cm. For the pixel in Fig. 13, the correlation between SMOS and the network was $R = 0.64$ with an RMSE of 0.08 $m^3\ m^{-3}$. On the other hand, note that there is essentially no correlation between SMOS soil moisture and τ in Fig. 13 for the 2014 and 2015 growing seasons. We did find a significant correlation of $R = -0.41$ for 2013. However, this correlation can be explained by a wet spring followed by a long dry-spell later in the summer such that low values of τ occurred during a period of high surface soil moisture and high values of τ in the middle of the growing season occurred during a period of low surface soil moisture. We find the same relationships for the two other SMOS pixels that overlap the South Fork in situ soil moisture network. Consequently, SMOS θ_v and τ products in Iowa do not appear to be correlated and therefore this idea cannot be used to explain the relationships between $\Delta\tau_v$ and precipitation shown in Fig. 12.

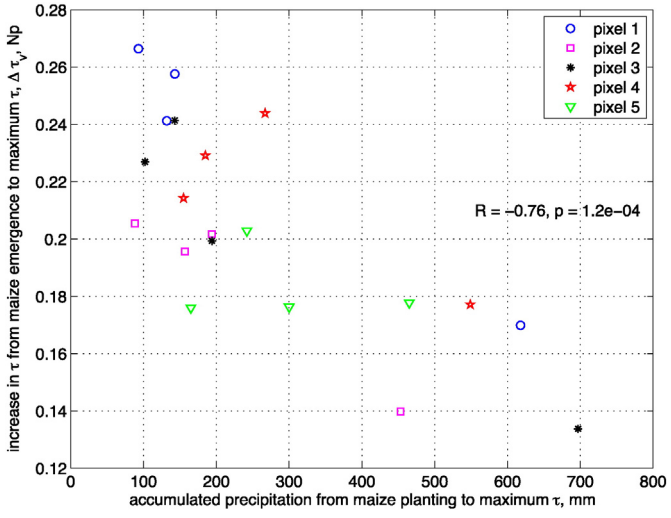

Fig. 12. The increase in SMOS τ from the time of maize emergence to the observed maximum value of τ, $\Delta\tau_v$, versus accumulated precipitation according to Daymet data during the same time period.

6.2. Other environmental factors affecting the magnitude of τ

The are other possible explanations for the observed differences in $\Delta\tau_v$ over the four years and among the five pixels. Perhaps peak M_w is not correlated with peak M_d and the relationship between dry matter and water in crops may be more complex and variable than what is illustrated by Fig. 5. While the accumulation of dry matter is known to be directly proportional to intercepted PAR as illustrated by Eq. (10), perhaps the ratio of M_w to M_d varies in response to environmental conditions and is more variable in rain-fed systems as compared to the irrigated system in our study. If in fact the ratio of M_w to M_d is conserved, if our meteorological data is representative of the five SMOS pixels, and if crops did not experience water stress (either from too little or too much water) during the four years we examined, then the observed variation in $\Delta\tau_v$ shown in Fig. 11 should be approximately the same as the observed variation in S in Table 4 according to Eq. (10) if fs and e are constant. However, we find that the correlation in Fig. 11 is low and has the wrong sign, and while $\Delta\tau_v$ varied between 0.13 to 0.27 Np or ±35%, S in Table 4 only varied from 3410 to 4870 MJ m^{-2} or ±18% (about half as much).

Another factor that could explain these observations is if f_S is indeed not constant in space and/or time. Under normal conditions, modern crops attain values of f_S approaching unity (Koester, Skoneczka, Cary, Diers, & Ainsworth, 2014). Management factors such as planting date, row width, and planting density can affect the timing and rate of canopy development and impact f_S. Temperature and precipitation can also impact f_S by affecting growth rate and developmental factors which determine when vegetative and reproductive growth occurs. Because f_S depends on growth it is actually also controlled to some extent by e. It has been shown that e has a range of observed values under field conditions (Zhu, Long, & Ort, 2010). In a meta-analysis conducted by Slattery & Ort (2015), observed values of e for maize were nearly double that of soybean but show similar ranges of magnitude.

Variability in available solar radiation (and therefore PAR) among growing seasons may be small as compared to variability in soil water, which influences crop growth in both positive and negative ways. Optimum values of soil water promote growth, while both extremely low and high values of soil water (as noted in Section 6.1) can inhibit growth. When soil water content decreases to the wilting point, roots are not able to draw water from the soil. The stomata of plants close in an effort to conserve water by decreasing transpiration. Since plants access CO_2 through the same stomata, photosynthesis and the assimilation of carbon decreases and so does the accumulation of dry matter, M_d. Water stress can reduce e by inducing stomatal closure and reducing the uptake of CO_2. Temperature affects e, with maximal values occurring at the optimum temperature for photosynthesis, which also varies between maize and soybean (Sage & Kubien, 2007).

6.3. Effect of the retrieval and smoothing algorithm on the magnitude of τ

Finally, the magnitude of the current SMOS τ product may be incorrect, and it is also possible that the smoothing method described in Section 2.1.1 adequately resolves the timing of the maximum values of τ but not its value. As noted earlier in Section 3.1, soil moisture retrieval from SMOS observations has been a higher priority, and as a result, adjustments to various parameters made to improve soil moisture statistics may have introduced errors in τ. In addition, the retrieval of θ_v and τ can only be as good as the model used in the estimation process. At present the retrieval process is not optimized for maize and soybean but for generic vegetation with M_w low enough for which soil moisture retrievals can be made. Before more work on interpreting

Please cite this article as: Hornbuckle, B.K., et al., SMOS optical thickness changes in response to the growth and development of crops, crop management, and weather, *Remote Sensing of Environment* (2016), http://dx.doi.org/10.1016/j.rse.2016.02.043

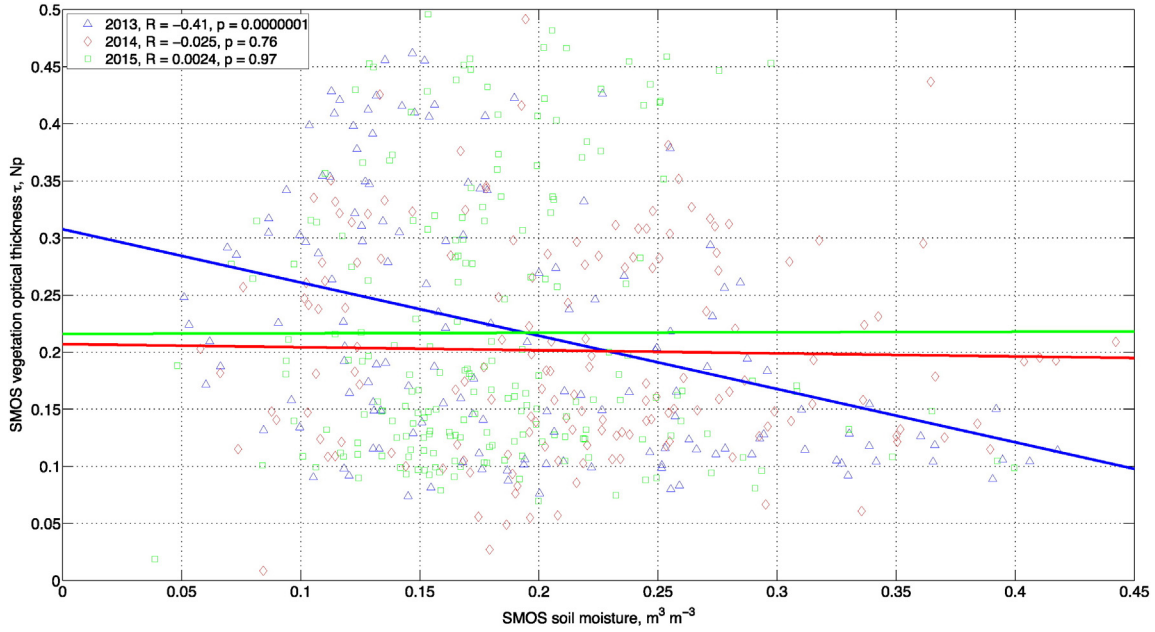

Fig. 13. The relationship between SMOS soil moisture and SMOS τ for a pixel in central Iowa (DGG 200057) between April and October for 2013–2015. This pixel encompasses much of the extent of an in situ soil moisture network in the watershed of the South Fork Iowa River. The colors correspond to the three years during with this in situ network has been in operation. (For interpretation of the references to color in this figure legend, the reader is referred to the web version of this article.)

SMOS τ is attempted, it may be useful to generate crop-specific values of τ using crop-specific values of ω (like that for forests (Rahmoune et al., 2013)). Efforts should also be made to refine the SMOS retrieval process in order to eliminate or at least reduce the noise in τ.

7. Conclusions

The SMOS Level 2 retrieval algorithm simultaneously estimates over land areas both soil moisture and τ, the optical thickness of vegetation, from observed L-band brightness temperature. The τ parameter has been shown to be directly proportional to vegetation water column density, M_w, the mass of water contained within vegetation tissue per ground area (also called VWC in the literature). We used a smoothing technique to remove large day-to-day variations in SMOS Level 2 τ that do not appear to be caused by natural factors. The resulting τ has a distinct shape in the U.S. Corn Belt that mirrors the annual growth and development of crops. SMOS τ increases after crops are planted, reaches a peak value, and then decreases as crops senesce and lose water.

We were able to explain the timing of the annual peak value of the smoothed τ signal and its variation over a four-year period by examining SMOS pixels in the Corn Belt state of Iowa for which the fraction of cropland was between 75 and 85%. Approximately 60% of these cropped areas were planted in maize (corn) and the balance in soybean. We found that the day of year on which the maximum value of SMOS Level 2 τ occurred was positively correlated ($R = 0.81$ and $p = 1.5\times10^{-5}$) with the day of year on which 50% of maize fields within the pixel had reached the third reproductive stage of development (R3 or "milk"). We also found that the day of peak τ was positively correlated with the day on which 1000°C day growing degree days had accumulated after maize planting ($R = 0.73$ and $p = 2.6\times10^{-21}$).

We hypothesized that the magnitude of the change in SMOS τ, $\Delta\tau_v$, defined as the difference between the peak value of τ and the value of τ at maize emergence, would be related to the amount of solar radiation (and therefore PAR) accumulated during the same time period. Our hypothesis assumed that crops accumulate more M_w in proportion to dry matter which is correlated to accumulated PAR. However, this hypothesis was not supported by our data. On the other hand, we found that $\Delta\tau_v$ was smallest for the year in which the most precipitation fell. This could be due to the fact that SMOS τ is a function of both vegetation and soil surface roughness. Soil surface roughness decreases with precipitation, and soil surface roughness may have been reduced the most during this wet year. However, the total change in soil surface roughness over a growing season will also depend on the type and timing of crop management activities such as tillage, planting, and fertilization, all of which disturb the soil surface.

Our work is significant for the following reasons. First, SMOS Level 2 τ could be used to monitor the growth and development (phenology) of crops and thus be used to estimate the timing of harvest and potentially crop yield. Currently the USDA uses ground-based visual surveys to report crop development in Crop Reporting Districts. In Iowa, these districts encompass 10 or more SMOS pixels. Hence SMOS τ could improve the spatial resolution of estimates of crop development by a factor of 10. Increasingly, crop models are being used within climate models to better simulate exchanges of energy and moisture between the land surface and the atmosphere that are modulated by annual changes in vegetation. In order for a crop model to provide a benefit over static vegetation, the timing of the growth and senescence of annual crops must be captured correctly. For example, Levis et al. (2012) based the time of planting on the accumulation of growing degree days starting on an arbitrary day in the spring. However, actual planting dates depend on other environmental factors (e.g., soil moisture which determines whether agricultural equipment can get into the field) and human decisions. Satellite estimates of crop development could be assimilated into crop models to determine whether actual crop development has been estimated correctly or not.

Second, SMOS Level 2 τ could be used as a measure of changes in vegetation that is distinct and yet complementary to traditional vegetation indices. While the spatial resolution of SMOS τ is quite large (about 40 km), L-band radiation emitted by the soil passes through the entire canopy and hence represents the integrated effect of the entire canopy (stems and leaves) in contrast to visible and near-infrared vegetation indices which are only sensitive to the very top of the canopy (upper-most leaves). This sensitivity to the entire vegetation canopy may prove key in the Corn Belt and other agricultural regions as commercial-scale cellulosic biorefineries become more common. These biorefineries, in contrast to grain ethanol production plants, are fueled by stover, the "leftover" plant material (stems and leaves) normally left in the field after harvest.

Please cite this article as: Hornbuckle, B.K., et al., SMOS optical thickness changes in response to the growth and development of crops, crop management, and weather, *Remote Sensing of Environment* (2016), http://dx.doi.org/10.1016/j.rse.2016.02.043

ARTICLE IN PRESS

SMOS Level 2 τ has the potential to produce timely and accurate estimates of the total production of crop biomass over the growing season, and hence crop stover. This data could be key to meeting bioenergy production goals (Perlack et al., 2005).

Third, SMOS Level 2 τ can be more rigorously justified from a theoretical standpoint than τ produced using observations from higher frequency satellite radiometers. The model most commonly used to interpret terrestrial brightness temperature is a zero-order solution of radiative transfer in vegetation. The zero-order solution is only valid when scattering within the canopy is small. Scattering depends on the electrical size of canopy components (stems, leaves, reproductive organs), the size of these components relative to the wavelength of radiation. Scattering becomes more significant as the electrical size of potential scatterers increases. For SMOS, $\lambda = 21$ cm, which is about a factor of 10 larger than the width of stems and leaves of crops like maize and soybean. On the other hand, the wavelength used by Jones et al. (2011) at 18.7 GHz is $\lambda = 1.60$ cm. Hence the simpler zero-order solution is much more likely to be valid at L-band than at other microwave frequencies currently available from existing satellite radiometers.

Future research on SMOS Level 2 τ will need to focus on determining the relationship between M_w and M_d, the mass of dry vegetation per ground area (which can be predicted with existing crop models), and will likely have to do so in a crop-specific manner. To our best knowledge, this can only be resolved by conducting empirical experiments under a range of environmental conditions for each crop of interest. Future investigations must also implement modeling frameworks capable of simulating the effects of crop management and the environment on f_S, the fraction of solar radiation intercepted by crops, and e, the radiation use efficiency of crops. The complex relationships that ultimately determine crop growth are difficult to resolve if only statistical relationships are considered. However, mechanistic photosynthesis models such as those based on the Farquhar, von Caemmerer, & Berry (1980) biochemical model are powerful tools for resolving the effects of environmental factors on plant growth (Bernacchi et al., 2013). Agro-ecosystem models that incorporate both management and environmental factors (e.g., Kucharik, 2003) are an example of the logical next step in addressing variations in $\Delta\tau_v$ as they relate to M_w and M_d and changes in soil surface roughness.

Finally, the SMOS Level 2 τ product itself needs to be improved. It is not known how much of the observed noise in τ is due to diurnal variations in M_w and how much is caused by other factors. Perhaps a first step would be to use crop-specific parameters in the retrieval process. It will also be necessary to quantitatively validate τ at the satellite scale to the same degree as SMOS soil moisture.

Acknowledgments

The authors received support from: NASA Earth and Space Sciences Fellowship NNX11AL44H; grant G11AP20079-2016IA265B from the Iowa Water Center, a Water Resources Research Institute administered by the USGS; and the Department of Agronomy at Iowa State University. The authors also appreciate the constructive comments made by the reviewers. This research was performed as part of Iowa Agriculture and Home Economics Experiment Station project IOW05387.

References

Abendroth, L. J., Elmore, R. W., Boyer, M. J., & Marlay, S. K. (2011). Corn growth and development. *Tech. Rep. PMR 1009*. Ames, IA: Iowa State University Extension.

Anderson, M. C., Norman, J. M., Meyers, T. P., & Diak, G. D. (2000). An analytical model for estimating canopy transpiration and carbon assimilation fluxes based on canopy light-use efficiency. *Agricultural and Forest Meteorology*, *101*, 265–289.

Bernacchi, C. J., Bagley, J. E., Serbin, S. P., Ruiz–Vera, U. M., Rosenthal, D. M., & Vanloocke, A. (2013). Modelling C3 photosynthesis from the chloroplast to the ecosystem. *Plant, Cell & Environment*, *36*(9), 1641–1657.

Bircher, S., Skou, N., & Kerr, Y. H. (2013). Validation of SMOS L1C and L2 products and important parameters of the retrieval algorithm in the Skjern River Catchment, western Denmark. *IEEE Transactions on Geoscience and Remote Sensing*, *51*(5), 2969–2985.

Boryan, C., Yang, Z., Mueller, R., & Craig, M. (2011). Monitoring US agriculture: The US Department of Agriculture, National Agricultural Statistics Service, Cropland Data Layer program. *Geocarto International*, *26*(5), 341–358.

Campbell, G. S., & Norman, J. M. (1998). *An introduction to environmental biophysics*. New York: Springer–Verlag.

Choudhury, B. J., Schmugge, T. J., Chang, A., & Newton, R. W. (1979). Effect of surface roughness on the microwave emission from soils. *Journal of Geophysical Research*, *84*, 5699–5706.

Connor, D. J., Loomis, R. S., & Cassman, K. G. (2011). *Crop ecology: Productivity and management in agricultural systems*. New York: Cambridge University Press.

Entekhabi, D., Njoku, E. G., O'Neill, P. E., Kellogg, K. H., Crow, W. T., Edelstein, W. N., ... Van Zyl, J. (2010). The Soil Moisture Active Passive (SMAP) mission. *Proceedings of the IEEE*, *98*(5), 704–716.

Escorihuela, M. J., Chanzy, A., Wigneron, J. -P., & Kerr, Y. H. (2010). Effective soil moisture sampling depth of L-band radiometry: A case study. *Remote Sensing of Environment*, *114*(5), 995–1001.

Farquhar, G., von Caemmerer, S. v., & Berry, J. (1980). A biochemical model of photosynthetic CO_2 assimilation in leaves of C3 species. *Planta*, *149*(1), 78–90.

Grant, E., Buchanan, T., & Cook, T. (1957). Dielectric behavior of water at microwave frequencies. *The Journal of Chemical Physics*, *26*, 156–161.

Holmes, T. R. H., Drusch, M., Wigneron, J. -P., & de Jeu, R. A. M. (2008). A global simulation of microwave emission: Error structures based on output from ECMWF's operational integrated forecast system. *IEEE Transactions on Geoscience and Remote Sensing*, *46*(4), 846–856.

Hornbuckle, B. K., England, A. W., De Roo, R. D., Fischman, M. A., & Boprie, D. L. (2003). Vegetation canopy anisotropy at 1.4 GHz. *IEEE Trans. Geosci. Remote Sensing*, *41*(10), 2211–2223.

Hunt, K. P., Niemeier, J. J., da Cunha, L. K., & Kruger, A. (2011). Using cellular network signal strength to monitor vegetation characteristics. *IEEE Geoscience and Remote Sensing Letters*, *8*, 346–349.

Jackson, T. J., & Schmugge, T. J. (1991). Vegetation effects on the microwave emission of soils. *Remote Sensing of Environment*, *36*, 203–212.

Jackson, T. J., Bindlish, R., Cosh, M. H., Zhao, T., Starks, P. J., Bosch, D. D., ... Leroux, D. (2012). Validation of Soil Moisture and Ocean Salinity (SMOS) soil moisture over watershed networks in the U.S. *IEEE Trans. Geosci. Remote Sensing*, *50*(5), 1530–1543.

Jones, M. O., Jones, L. A., Kimball, J. S., & McDonald, K. C. (2011). Satellite passive microwave remote sensing for monitoring global land surface phenology. *Remote Sensing of Environment*, *115*, 1102–1114.

Kerr, Y. H., Waldteufel, P., Richaume, P., Davenport, I., Ferrazzoli, P., & Wigneron, J. -P. (2011, Dec). Algorithm theoretical basis document (ATBD) for the SMOS Level 2 soil moisture processor development continuation project. *Tech. Rep. SO-TN-ESL-SM-GS-0001, v3.g*. Toulouse, France: CESBIO.

Kerr, Y. H., Waldteufel, P., Richaume, P., Wigneron, J. P., Ferrazzoli, P., Mahmoodi, A., ... Delwart, S. (2012). The SMOS soil moisture retrieval algorithm. *IEEE Transactions on Geoscience and Remote Sensing*, *50*(5), 1384–1403.

Kerr, Y. H., Waldteufel, P., Wigneron, J. -P., Delwart, S., Cabot, F., Boutin, J., ... Mecklenburg, S. (2010). The SMOS mission: New tool for monitoring key elements of the global water cycle. *Proceedings of the IEEE*, *98*(5), 666–687.

Koester, R. P., Skoneczka, J. A., Cary, T. R., Diers, B. W., & Ainsworth, E. A. (2014). Historical gains in soybean (glycine max merr.) seed yield are driven by linear increases in light interception, energy conversion, and partitioning efficiencies. *J. Experiment. Botany*, *65*(12), 3311–3321.

Kucharik, C. J. (2003). Evaluation of a process-based agro-ecosystem model (Agro-IBIS) across the US Corn Belt: Simulations of the interannual variability in maize yield. *Earth Interactions*, *7*(14), 1–33.

Lawrence, H., Wigneron, J. -P., Richaume, P., Novello, N., Grant, J., Mialon, A., ... Kerr, Y. (2014). Comparison between SMOS vegetation optical depth products and MODIS vegetation indices over crop zones of the USA. *Remote Sensing of Environment*, *140*, 396–406.

Levis, S., Bonan, G. B., Kluzek, E., Thornton, P. E., Jones, A., Sacks, W. J., & Kucharik, C. J. (2012). Interactive crop management in the Community Earth System Model (CESM1): Seasonal influences on land–atmosphere fluxes. *Journal of Climate*, *25*, 4839–4859.

Liu, Y. Y., van Dijk, A. I. J. M., de Jeu, R. A. M., Canadell, J. G., McCabe, M. F., Evans, J. P., & Wang, G. (2015). Recent reversal in loss of global terrestrial biomass. *Nature Climate Change*, *5*, 470–474.

Monteith, J. L., & Moss, C. J. (1977). Climate and the efficiency of crop production in Britain [and discussion]. *Philosophical Transactions of the Royal Society of London B: Biological Sciences*, *281*(980), 277–294.

Njoku, E. G., & Chan, S. K. (2006). Vegetation and surface roughness effects on AMSR-E land observations. *Remote Sensing of Environment*, *100*, 190–199.

O'Neill, P., Chan, S., Njoku, E., Jackson, T., & Bindlish, R. (2015). Soil Moisture Active Passive (SMAP) algorithm theoretical basis document level 2 & 3 soil moisture (passive) data products. *Tech. Rep. JPL D-66480*. National Aeronautics and Space Administration (NASA) Jet Propulsion Laboratory (JPL).

Patton, J., & Hornbuckle, B. (2013). Initial validation of SMOS vegetation optical thickness over Iowa. *IEEE Geoscience and Remote Sensing Letters*, *10*(4), 647–651.

Patton, J. C. (2014). *Comparison of SMOS and SMAP vegetation optical thickness*. Ph.D. thesis Iowa State University of Science and Technology.

Pedersen, P. (2009). Soybean growth and development. *Tech. Rep. PMR 1945*. Ames, IA: Iowa State University Extension.

Perlack, R. D., Wright, L. L., Turhollow, A. F., Graham, R. L., Stokes, B. J., & Erbach, D. C. (2005). Biomass as feedstock for a bioenergy and bioproducts industry: The technical feasibility of a billion-ton annual supply. *Tech. rep.* (DTIC Document).

Rahmoune, R., Ferrazzoli, P., Kerr, Y. H., & Richaume, P. (2013). SMOS Level 2 retrieval algorithm over forests: Description and generation of global maps. *IEEE Journal*

Please cite this article as: Hornbuckle, B.K., et al., SMOS optical thickness changes in response to the growth and development of crops, crop management, and weather, *Remote Sensing of Environment* (2016), http://dx.doi.org/10.1016/j.rse.2016.02.043

ARTICLE IN PRESS

of Selected Topics in Applied Earth Observations and Remote Sensing, *6*(3), 1430–1439.

Rahmoune, R., Ferrazzoli, P., Kumar Singh, Y., Kerr, Y. H., Richaume, P., & Al Bitar, A. (2014). SMOS retrieval results over forests: Comparisons with independent measurements. *IEEE Journal of Selected Topics in Applied Earth Observations and Remote Sensing*, *7*(9), 3858–3865.

Ramsay, J. O., Wickham, H., Graves, S., & Hooker, G. (2013). FDA: Functional data analysis. *R package version 2.3.6*.

Rondinelli, W. J., Hornbuckle, B. K., Patton, J. C., Cosh, M. H., Walker, V. A., Carr, B. D., & Logsdon, S. D. (2015). Different rates of soil drying after rainfall are observed by the SMOS satellite and the South Fork in situ soil moisture network. *Journal of Hydrometeorology*, *16*, 889–903.

Rowlandson, T. L., Hornbuckle, B. K., Bramer, L. M., Patton, J. C., & Logson, S. D. (2012). Comparisons of evening and morning SMOS passes over the Midwest United States. *IEEE Transactions on Geoscience and Remote Sensing*, *50*(5), 1544–1555.

Sage, R. F., & Kubien, D. S. (2007). The temperature response of C3 and C4 photosynthesis. *Plant, Cell & Environment*, *30*(9), 1086–1106.

Schlenz, F., dall'Amico, J. T., Mauser, W., & Loew, A. (2012). Analysis of SMOS brightness temperature and vegetation optical depth data with coupled land surface and radiative transfer models in southern Germany. *Hydrology and Earth System Sciences*, *16*, 3517–3533.

Singer, J. W., Meek, D. W., Sauer, T. J., Prueger, J. H., & Hatfield, J. L. (2011). Variability of light interception and radiation use efficiency in maize and soybean. *Field Crops Research*, *121*, 147–152.

Slattery, R., & Ort, D. (2015). Photosynthetic energy conversion efficiency: Setting a baseline for gauging future improvements in important food and biofuel crops. *Plant Physiology*, *168*(2), 383–392.

Slatyer, R. S. (1967). *Plant–water relationships.* New York: Academic Press.

Thornton, P. E., Running, S. W., & White, M. A. (1997). Generating surfaces of daily meteorological variables over large regions of complex terrain. *Journal of Hydrology*, *190*, 214–251.

Thornton, P. E., Thornton, M. M., Mayer, B. W., Wilhelmi, N., Wei, Y., Devarakonda, R., & Cook, R. B. (2014). *Daymet: Daily surface weather data on a 1-km grid for North America, version 2.* (Available from Oak Ridge National Laboratory Distributed Active Archive Center, Oak Ridge, TN, USA).

Ulaby, F. T., & El-Rayes, M. A. (1987). Microwave dielectric spectrum of vegetation — part II: Dual-dispersion model. *IEEE Transactions on Geoscience and Remote Sensing, GE–25*(5), 550–557.

Ulaby, F. T., & Jedlicka, R. P. (1984). Microwave dielectric properties of plant materials. *IEEE Transactions on Geoscience and Remote Sensing, GE–22*(4), 406–415.

Ulaby, F. T., Moore, R. K., & Fung, A. K. (1981). *Microwave remote sensing: Active and passive. 1*, Norwood, MA: Artech House.

Wigneron, J. -P., Kerr, Y., Waldteufel, P., Saleh, K., Escorihuela, M. -J., Richaume, P., ... Schwank, M. (2007). L-band microwave emission of the biosphere (L-MEB) model: Description and calibration against experimental data sets over crop fields. *Remote Sensing of Environment*, *107*, 639–655.

Wigneron, J. -P., Laguerre, L., & Kerr, Y. H. (2001). A simple parameterization of the L-band microwave emission from rough agricultural soils. *IEEE Transactions on Geoscience and Remote Sensing*, *39*, 1697–1707.

Wigneron, J. -P., Schwank, M., Lopez Baeza, E., Kerr, Y., Novello, N., Millan, C., ... Mecklenburg, S. (2012). First evaluation of the simultaneous SMOS and ELBARA-II observations in the Mediterranean region. *Remote Sensing of Environment*, *124*, 26–37.

Zhu, X. -G., Long, S. P., & Ort, D. R. (2010). Improving photosynthetic efficiency for greater yield. *Annual Review of Plant Biology*, *61*, 235–261.

Zobeck, T. M., & Onstad, C. A. (1987). Tillage and rainfall effects on random roughness: A review. *Soil & Tillage Research*, *9*, 1–20.

Please cite this article as: Hornbuckle, B.K., et al., SMOS optical thickness changes in response to the growth and development of crops, crop management, and weather, *Remote Sensing of Environment* (2016), http://dx.doi.org/10.1016/j.rse.2016.02.043